Clinical & Translational Immunology

Australian and New Zealand Society for Immunology Inc.

Clinical & Translational Immunology 2021; e1300. doi: 10.1002/cti2.1300
www.wileyonlinelibrary.com/journal/cti

ORIGINAL ARTICLE

IL-33/ST2 axis deficiency exacerbates neutrophil-dominant allergic airway inflammation

Qiyun Ma[1], Yan Qian[1], Jingxian Jiang[1], Jingjing Wu[1], Meijuan Song[1], Xinyu Li[2], Zhongqi Chen[1], Zhengxia Wang[1], Ranran Zhu[1], Zhixiao Sun[1], Mao Huang[1], Ningfei Ji[1] & Mingshun Zhang[2]

[1]Department of Respiratory and Critical Care Medicine, The First Affiliated Hospital of Nanjing Medical University, Nanjing, China
[2]NHC Key Laboratory of Antibody Technique, Jiangsu Key Laboratory of Pathogen Biology, Department of Immunology, Nanjing Medical University, Nanjing, China

Correspondence
M Huang and N Ji, Department of Respiratory and Critical Care Medicine, The First Affiliated Hospital of Nanjing Medical University, Nanjing 210029, China.
E-mails: hm6114@163.com (MH); jiningfei@163.com (NJ)

M Zhang, NHC Key Laboratory of Antibody Technique, Jiangsu Key Laboratory of Pathogen Biology, Department of Immunology, Nanjing Medical University, Nanjing 211166, China.
E-mail: mingshunzhang@njmu.edu.cn

Received 15 September 2020;
Revised 30 April and 27 May 2021;
Accepted 27 May 2021

doi: 10.1002/cti2.1300

Clinical & Translational Immunology
2021; **10**: e1300

Abstract

Objective. The IL-33/ST2 axis has been extensively investigated in type 2 eosinophilic inflammation. Here, we aimed to investigate the role of the IL-33/ST2 axis in neutrophil-dominant allergic airway inflammation. **Methods.** House-dust mite (HDM) extract and lipopolysaccharide (LPS) were administered to establish a murine model of neutrophil-dominant allergic airway inflammation. The formation of neutrophilic extracellular traps (NETs) in the lung tissues was demonstrated by immunofluorescence imaging. Mature IL-33 in bronchoalveolar lavage fluid (BALF) was detected by Western blotting. The neutrophilic chemokine KC produced by bone marrow-derived macrophages (BMDMs) or primary alveolar epithelial cells was measured with a commercial ELISA kit. **Results.** In the present study, we observed neutrophilic inflammation and tight junction damage in the lungs of mice sensitised with HDM and LPS. Furthermore, sensitisation with HDM and LPS resulted in the formation of NETs, accompanied by increased levels of mature IL-33 in the BALF. Moreover, LPS damaged the epithelial tight junction protein occludin directly or indirectly by inducing NET formation. Surprisingly, IL-33 deficiency augmented neutrophilia and epithelial barrier injury in the lungs of mice after sensitisation with HDM and LPS. Similarly, the absence of ST2 exacerbated the neutrophilic inflammatory response, decreased the expression of occludin and exacerbated the severity of neutrophil-dominant allergic airway inflammation in an HDM/LPS-induced mouse model. Mechanistically, BMDMs and alveolar epithelial cells from IL-33- or ST2-deficient mice tended to produce higher levels of the neutrophilic chemokine KC. **Conclusions.** These results demonstrated that the IL-33/ST2 axis may play a protective role in neutrophil-dominant allergic airway inflammation.

Keywords: animal models, asthma, barrier, epithelium, inflammation

INTRODUCTION

Allergic asthma is a common respiratory disease characterised by airway inflammation, airway remodelling and airway hyperresponsiveness. It has been reported that distinct inflammatory patterns of eosinophilic, mixed, neutrophilic and paucigranulocytic cells can be seen in the airways of asthmatic patients.[1] Neutrophilic inflammation presents in approximately half of the patients with asthma who are poorly responsive to corticosteroid therapy and is associated with more severe asthma.[1–3]

In response to inflammatory stimuli, neutrophils undergo specific cell death and form web-like structures called neutrophilic extracellular traps (NETs).[4] NETs are composed of chromatin complexes of cell-free DNA and citrullinated histones decorated with neutrophilic granular proteins, such as neutrophilic elastase (NE) and myeloperoxidase (MPO).[4] NETs play an important role in host defence, and these structures are also associated with tissue damage.[5] Several recent studies have revealed that NETs, which are associated with disease severity, are increased in a subset of patients with severe asthma.[6,7]

The airway epithelium is the first physical barrier that protects against inhaled allergens and pathogens. Various environmental factors and inflammatory cytokines can impair the airway epithelial barrier.[8–10] Meanwhile, increased damage might allow more allergens, microbes and pollutants to penetrate the epithelium, which results in activation of the immune system and the development and exacerbations of asthma.[10] Several recent studies have revealed that the barrier function of epithelium and tight junction (TJ) molecule expression are impaired in asthma.[11–13] Subsequently, bulk plasma proteins leak through the microvascular–epithelial barrier in asthmatic patients, which is especially pronounced in patients with severe and exacerbating asthma.[14]

Interleukin-33 (IL-33) is a chromatin-associated nuclear cytokine from the IL-1 family that is normally released by damaged or necrotic barrier cells, including endothelial and epithelial cells, functioning as an alarmin.[15,16] It has been demonstrated that inflammatory proteases from neutrophils can process full-length IL-33 into shorter mature forms that are 10- to 30-fold more potent than the full-length form in activating target cells.[17,18] IL-33 exerts its cytokine effects by binding to its receptor ST2 (suppression of tumorigenicity 2), which results in the activation of intracellular signalling pathways.[16] The IL-33/ST2 axis has been found to play a vital role in type 2 response. Serum levels of sST2 (soluble ST2, a decoy receptor for IL-33) are significantly increased in lung diseases characterised by neutrophilic inflammation (e.g. chronic obstructive lung disease and pneumonia)[19,20] and are associated with the severity and exacerbation of asthma.[21,22] However, the role of the IL-33/ST2 axis in neutrophil-dominant allergic airway inflammation remains unclear. In the present study, we demonstrated that IL-33/ST2 deficiency can augment neutrophilic inflammation and epithelial barrier damage in a murine model of HDM/LPS-induced neutrophil-dominant allergic airway inflammation, suggesting that the IL-33/ST2 axis may have a protective function in a subset of cases of severe asthma with neutrophilic airway inflammation.

RESULTS

HDM/LPS induced airway inflammation and injured the epithelial barrier

The environmental allergen HDM is an important cause of allergic inflammation in asthma, and LPS exposure is associated with the severity and exacerbation of asthma.[23,24] Moreover, coexposure to HDM and LPS has been used to establish neutrophil-dominated airway inflammation models that simulate severe asthma.[25,26] Accordingly, we developed a murine model of neutrophil-dominant allergic airway inflammation in which mice were sensitised by coexposure to HDM and LPS for 3 days followed by the rest for 4 days and then challenged by HDM alone for 8 days (Figure 1a). As shown in Figure 1b and c, the levels of total IgE and HDM-specific IgE in serum were drastically higher in the severe group (sensitised with HDM and LPS) than in the common group (sensitised with HDM alone). Similarly, lung histological analysis showed increased inflammatory cell infiltration (Figure 1d) and goblet cell hyperplasia (Figure 1e) in the lungs of mice treated with HDM/LPS. Meanwhile, the TJ protein occludin, which contributes to TJ stabilisation and optimal barrier function,[27] was significantly decreased in the lungs of mice treated with HDM/LPS (Figure 1f and g). In addition, the expression of another TJ protein

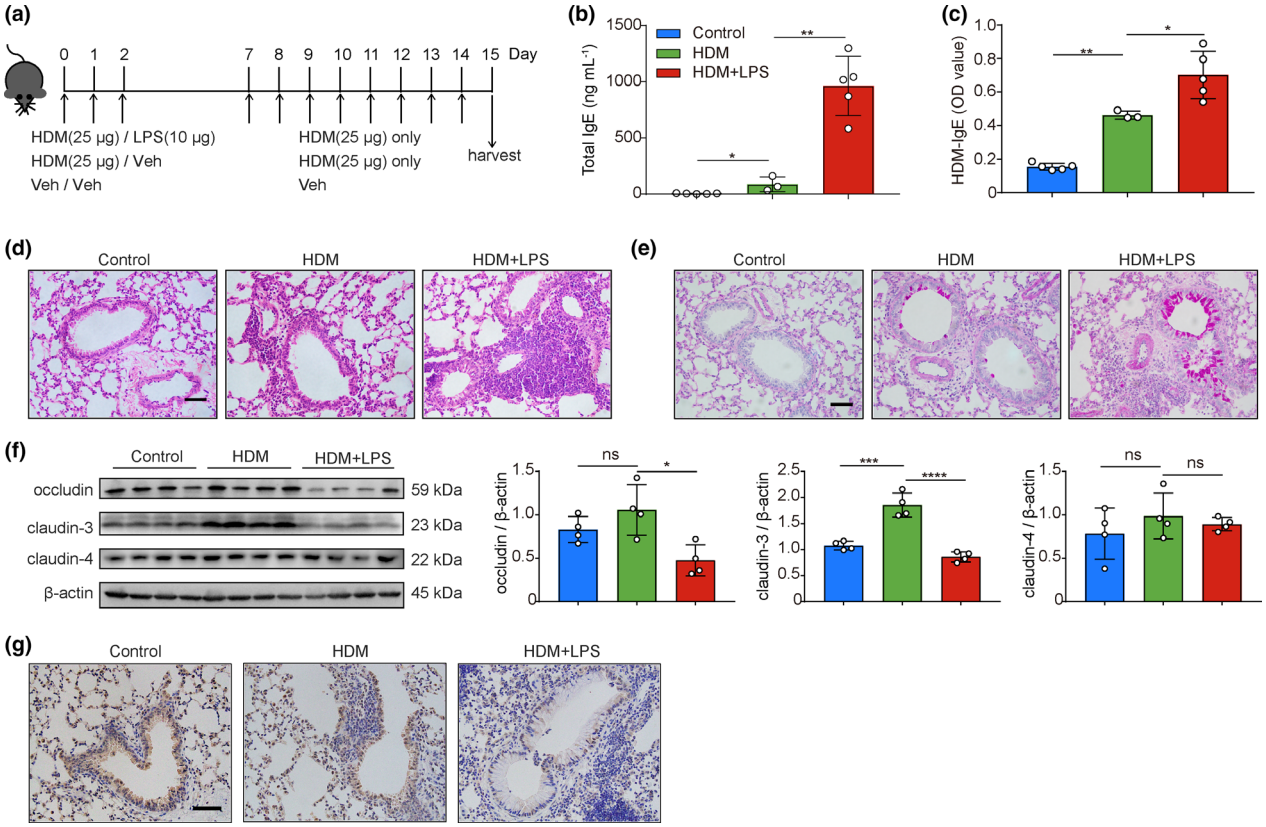

Figure 1. Neutrophilic inflammation and impaired tight junctions in HDM/LPS-induced neutrophil-dominant allergic airway inflammation model. Shown are representative results from two independent experiments with 3, 4 or 5 mice per group. **(a)** Schematic diagram of the murine model protocol. Mice were treated with HDM/LPS, HDM or PBS via oropharyngeal aspiration (OPA) during sensitisation, followed by HDM or PBS challenge. **(b, c)** The levels of total IgE **(b)** and HDM-IgE **(c)** in the serum were measured by ELISA. **(d)** Representative images of histological lung sections stained with haematoxylin and eosin (H&E) to evaluate the infiltration of inflammatory cells. **(e)** Representative images of histological lung sections stained with periodic acid–Schiff (PAS) to analyse goblet cell hyperplasia. **(f)** Tight junction protein (occludin, claudin-3 and claudin-4) expression was measured by Western blotting, and the repeated results were confirmed by greyscale analysis. **(g)** Representative images of immunohistochemical staining for occludin expression in the lung. Original magnification 400×; scale bar, 50 μm. Bar graphs and data are presented as the mean ± SD. *$P < 0.05$, **$P < 0.01$, ***$P < 0.001$ and ****$P < 0.0001$. ns, not significant.

family member,[28] claudin-3, was upregulated in the lungs of mice treated with HDM alone but decreased in mice treated with HDM/LPS (Figure 1f). However, the expression of claudin-4 in the lung was comparable among the three groups (Figure 1f). Collectively, these results indicated that HDM and LPS induced elevated airway inflammation and damaged lung epithelial tight junctions in a murine model of neutrophil-dominant allergic airway inflammation.

HDM and LPS augmented neutrophilic inflammation and induced NET formation during the sensitisation phase

To further address the roles of HDM and LPS at the early stage of allergic airway inflammation development, mice were sensitised with HDM and LPS, HDM alone or PBS as a vehicle control for 3 days and sacrificed after 24 h (Figure 2a). After sensitisation, the number of total inflammatory cells in the airways of HDM/LPS-treated mice was significantly increased, primarily attributed to the recruitment of neutrophils instead of eosinophils (Figure 2b). In addition to elevated neutrophilic inflammation, the transcript level of neutrophilic chemokine KC and the protein level of monocyte chemokine MCP-1 were increased in the lungs of HDM/LPS-treated mice (Figure 2c). In addition, the levels of the proinflammatory cytokines IL-1β, TNF-α and IL-6 were higher in the lungs of HDM/LPS-treated mice, although the difference in TNF-α levels was not statistically significant (Figure 2e). In contrast, the levels of the eosinophilic

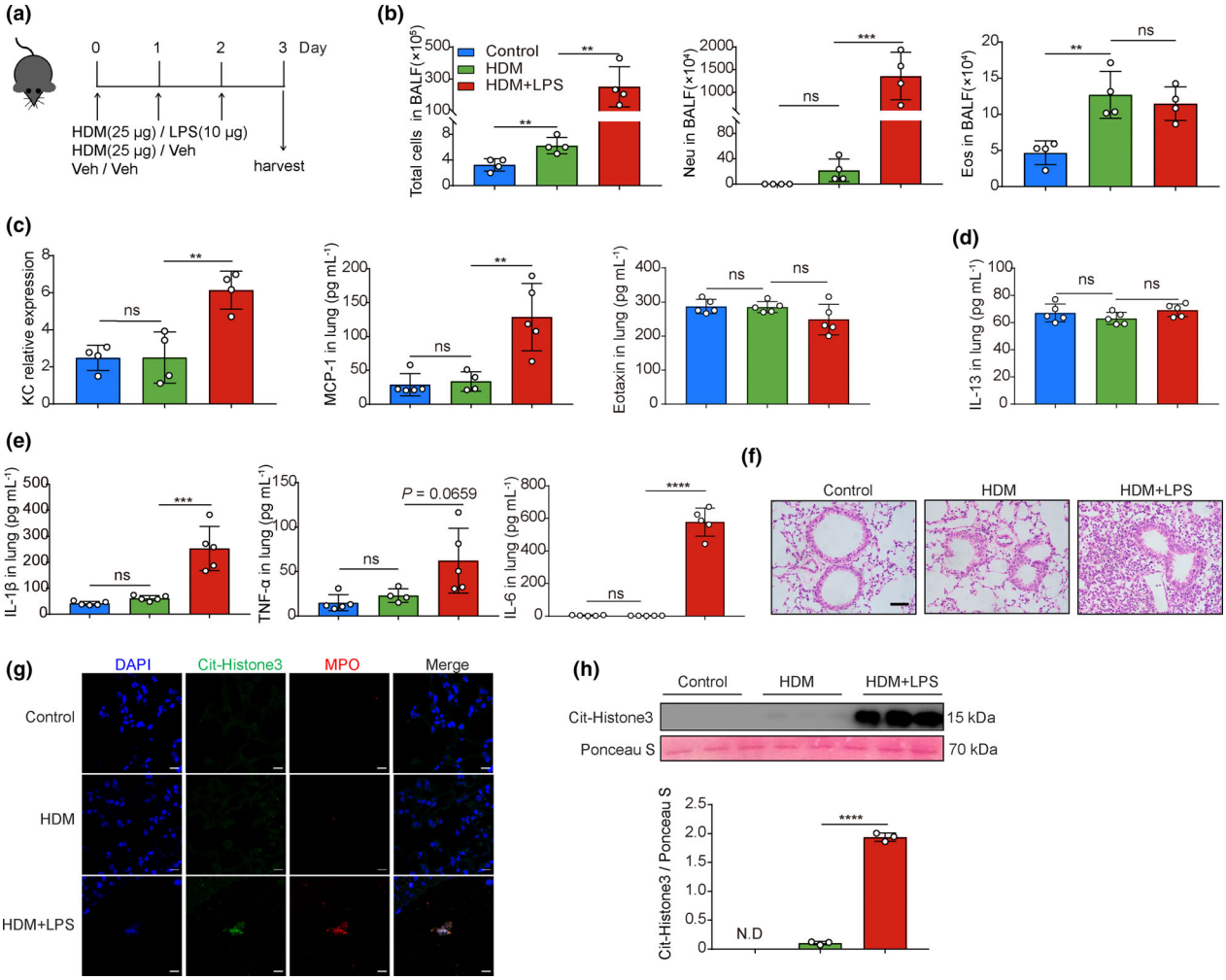

Figure 2. HDM and LPS potentiated neutrophilic inflammation and NET formation during sensitisation. Shown are representative results from two independent experiments with 3, 4 or 5 mice per group. **(a)** Scheme of allergen sensitisation model protocol. The mice were treated with HDM/LPS, HDM or PBS and were sacrificed at day 3. **(b)** The numbers of total cells, neutrophils (Neu) and eosinophils (Eos) in bronchoalveolar lavage fluid (BALF) were determined by flow cytometry. **(c)** The mRNA level of neutrophilic chemokine (KC) and the protein levels of monocyte chemokine (MCP-1) and eosinophilic chemokine (eotaxin) in the lung were evaluated by qPCR and ELISA respectively. **(d)** The level of IL-13 and **(e)** the levels of inflammatory cytokines (IL-1β, TNF-α and IL-6) in the lung were evaluated by ELISA. **(f)** Representative images of histological lung sections stained with H&E for evaluating infiltration of inflammatory cells; original magnification 400×; scale bar, 50 μm. **(g)** Neutrophilic extracellular traps (NETs) in the lung were identified as costained with DAPI (blue), cit-Histone3 (green) and MPO (red) and observed by confocal microscopy; original magnification 630×; scale bar, 10 μm. **(h)** Cit-Histone3 was measured by Western blotting and Ponceau S staining as a loading control to assess the level of NETs in the BALF; N.D, not detected. Bar graphs and data are presented as the mean ± SD. $^{**}P < 0.01$, $^{***}P < 0.001$ and $^{****}P < 0.0001$. ns, not significant.

chemokine eotaxin (Figure 2c) and the type 2 inflammation-related cytokine IL-13 (Figure 2d) were not changed. The exacerbated lung inflammation in HDM/LPS-sensitised mice was further demonstrated by lung histological analysis (Figure 2f).

Previous studies have reported that introducing LPS into the mouse airway could induce NET formation.[26,29] NETs can be identified by colocalisation of cell-free DNA, citrullinated histone H3 (cit-Histone3) and myeloperoxidase (MPO) using immunofluorescence microscopy. As shown in immunofluorescence images (Figure 2g), NETs could be observed in the lungs of HDM- and LPS-treated mice but not PBS- or HDM-treated mice. Similarly, cit-Histone3 in the BALF of coexposed mice was significantly elevated (Figure 2h). Together, these above findings

suggested that coexposure to allergens and LPS during sensitisation resulted in augmented neutrophilic inflammation and NET formation.

Impaired lung epithelial barrier function and elevated IL-33 maturation occurred at the early stage of the neutrophil-dominant allergic airway disease

Given that epithelial barrier function may be associated with allergen permeation, which may subsequently affect the development of asthma, we next examined whether lung epithelial barrier function was damaged after sensitisation with the combination of HDM and LPS. Total protein levels in the BALF of HDM/LPS-treated mice were increased (Figure 3a), which reflected elevated lung epithelial permeability. To study this further, fluorescein isothiocyanate–dextran 4 (FITC–dextran 4, FD4) was intratracheally instilled into mouse airways, and an hour later, serum was collected to determine the leakage of FD4 from airways to blood vessels. As expected, compared with the PBS control group, the fluorescence intensity of FD4 in the serum of the HDM/LPS group was higher, whereas a statistically significant increase was not observed in the HDM-alone-treated group (Figure 3b). In addition, the expression of occludin was reduced in the lung tissues from mice sensitised with HDM and LPS, as evidenced by Western blotting analysis (Figure 3c) and further demonstrated by immunohistochemistry (Figure 3d).

Lipopolysaccharide stimulation can trigger lung epithelial cells to release alarmin IL-33, which plays an important role in asthma.[30] In our study, however, lung IL-33 levels were comparable between the HDM/LPS and HDM-alone groups (Figure 3e). As the cytokine activity of the mature form of IL-33 was more potent than that of the full-length form, mature form IL-33 expression in BALF was detected by Western blotting. As shown

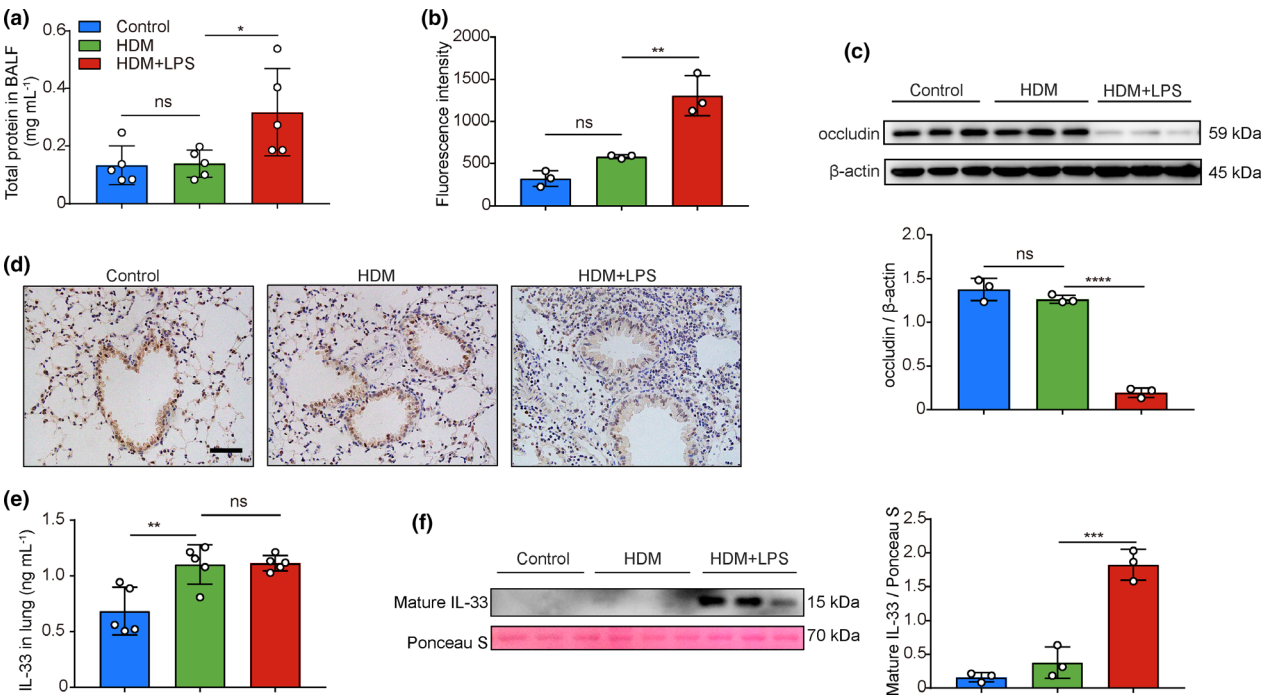

Figure 3. HDM and LPS promoted tight junction injury and IL-33 maturation during allergen sensitisation. Shown are representative results from two independent experiments with 3 or 5 mice per group. **(a)** Total protein contents in BALF were determined by the Bradford protein assay. **(b)** The fluorescence intensity of fluorescein isothiocyanate–dextran (FD4) in the serum was determined to assess pulmonary epithelial permeability. **(c)** The expression of tight junction protein (occludin) was measured by Western blotting. **(d)** Representative images of immunohistochemical staining for analysis of occludin expression; original magnification 400×; scale bar, 50 μm. **(e)** The level of IL-33 (containing both the full-length form and the mature form) in the lung was detected by ELISA. **(f)** The level of the mature form of IL-33 in BALF was measured by Western blotting, and Ponceau S stain was used as a loading control. Bar graphs and data are presented as the mean ± SD. $*P < 0.05$, $**P < 0.01$, $***P < 0.001$ and $****P < 0.0001$. ns, not significant.

in Figure 3f, combination treatment with HDM and LPS caused significantly higher levels of the mature form of IL-33 in BALF than in PBS or HDM alone. Thus, these findings revealed that coexposure to allergens and LPS may damage lung epithelial barrier function and promote IL-33 maturation at the early stage of neutrophil-dominant allergic airway disease development.

LPS and NETs decreased the epithelial cell tight junction protein occludin *in vitro*

Previous data confirmed that lung epithelial barrier function injury occurred after allergen sensitisation in the presence of LPS. *In vitro*, we stimulated the murine lung epithelial cell line MLE-12 with LPS to explore whether LPS could damage lung epithelial tight junctions directly. As shown in Figure 4a, LPS reduced the expression of occludin on lung epithelial cells. To further decipher the molecular mechanisms, we detected the activation level of NF-κB in MLE-12 cells following LPS stimulation. We found that NF-κB was activated in LPS-treated MLE-12 cells within a short time (Figure 4b). As expected, the deleterious effects of LPS on MLE-12 cell tight junctions could be rescued by an inhibitor of NF-κB (Figure 4c). Similarly, LPS decreased occludin expression in the human bronchial epithelial cell line 16HBE by activating NF-κB signalling (Figure 4d–f). In short, the above results indicated that LPS exposure directly decreased lung

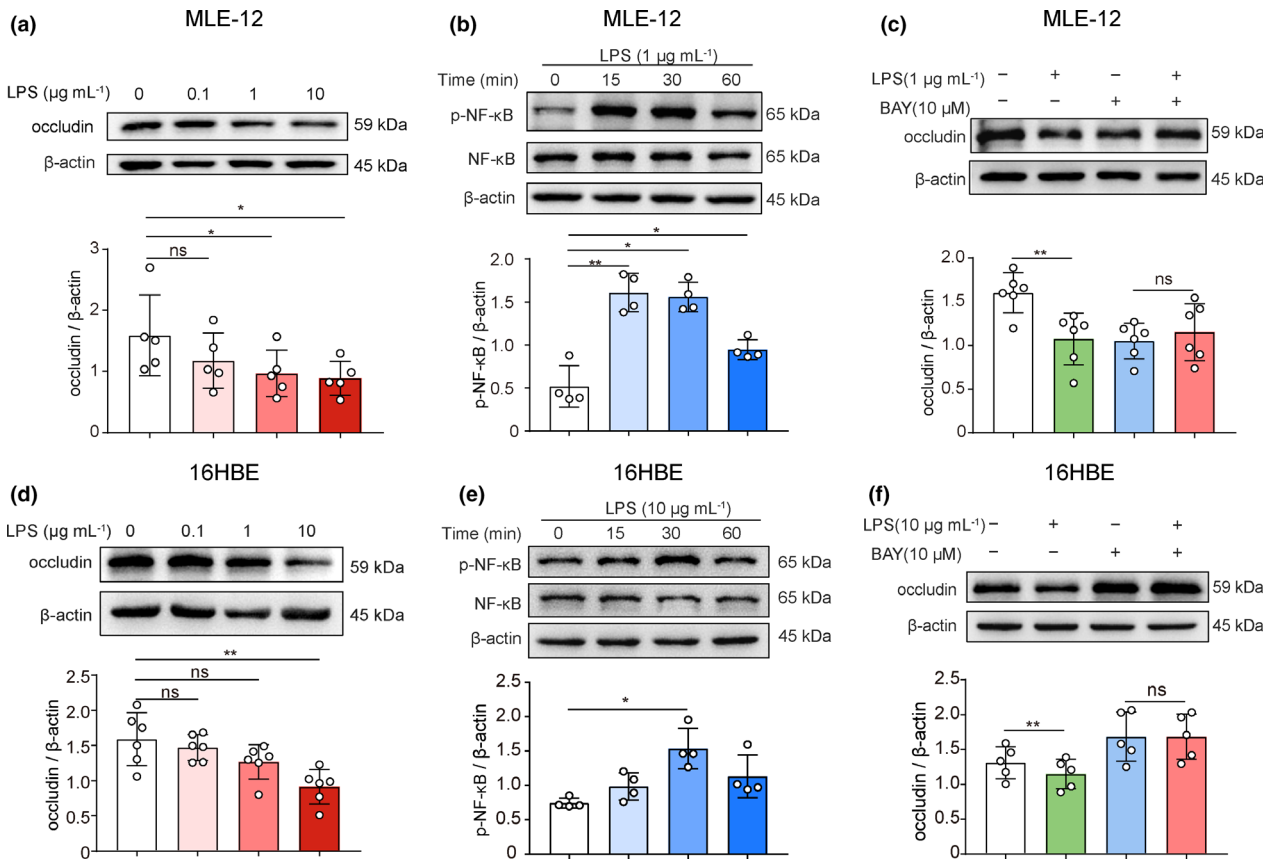

Figure 4. LPS damaged the tight junctions of lung epithelial cells directly via NF-κB signalling. **(a)** Occludin expression in MLE-12 cells treated with different doses of LPS for 24 h was measured by Western blotting (n = 5). **(b)** MLE-12 cells were treated with LPS (1 μg mL^{-1}) for 15, 30 or 60 min, and the levels of NF-κB and p-NF-κB were analysed by Western blotting (n = 4). **(c)** MLE-12 cells were pretreated with an inhibitor of NF-κB (BAY, 10 μM) for 60 min followed by stimulation with LPS (1 μg mL^{-1}) for 24 h, and the expression of occludin was analysed by Western blotting (n = 6). **(d)** Occludin expression in 16HBE cells treated with different doses of LPS for 24 h was measured by Western blotting (n = 6). **(e)** 16HBE cells were treated with LPS (10 μg mL^{-1}) for 15, 30 or 60 min, and the levels of NF-κB and p-NF-κB were analysed by Western blotting (n = 4). **(f)** 16HBE cells were pretreated with an inhibitor of NF-κB (BAY, 10 μM) for 60 min followed by stimulation with LPS (10 μg mL^{-1}) for 24 h, and the expression of occludin was analysed by Western blotting (n = 5). Bar graphs and data are presented as the mean ± SD. *P < 0.05 and **P < 0.01. ns, not significant.

epithelial cell tight junction protein occludin via the NF-κB signalling pathway.

As NETs developed in the mice treated with HDM and LPS (Figure 2g and h), we then addressed whether LPS could induce NET formation and subsequently result in tight junction disorder. To verify this possibility, mouse bone marrow neutrophils were stimulated with LPS in serum-free culture media, and NET formation was observed by confocal macroscopy. In line with some previous studies,[31] LPS alone was able to induce NET formation *in vitro* (Figure 5a and b). Furthermore, we exposed MLE-12 cells to NET-rich supernatant for 24 h and found that occludin expression on epithelial cells was decreased (Figure 5c). Considering that the decrease in tight junction proteins may be attributed to NET-associated proteases, we evaluated whether inhibitors of neutrophilic elastase (NE) or MMP-9 could rescue occludin expression. Of note, the reduction in occludin expression in MLE-12 cells could be largely rescued by pretreating NET-rich supernatant with the inhibitor of NE (sivelestat) but not with the inhibitor of MMP-9 (MMP-9-IN-1) (Figure 5d and e). Together, the above results suggested that NETs could damage the murine lung epithelial cell tight junction protein occludin *in vitro*. To further verify these findings in human lung epithelial cells, 16HBE, A549 and H1975 cells were treated with NET-rich media induced from human blood neutrophils. Unexpectedly, occludin expression was upregulated in 16HBE cells by NETs (Figure 5f). In contrast, the effects of NETs on A549 and H1975 cells were consistent with MLE-12 cells (Figure 5g and h). Likewise, sivelestat and MMP-9-IN-1 were used to investigate whether the effect of NETs on 16HBE and A549 cells relied on elastase or MMP-9. However, neither sivelestat nor MMP-9-IN-1 restored occludin expression (Figure 5i–l). Taken together, these findings indicated that NET formation following LPS exposure could disrupt tight junction protein expression in lung epithelial cells.

IL-33 deficiency aggravated airway neutrophilic inflammation and promoted lung epithelial barrier injury during allergen sensitisation

As evidenced by the above findings, the mature form IL-33 contents in the BALF were significantly higher after sensitisation with the combination of allergen HDM and LPS (Figure 3f). To explore the role of IL-33 in the development of neutrophil-dominant allergic airway disease, we used HDM and LPS coexposure models for 3 days by oropharyngeal aspiration in wild-type (WT) and IL-33-deficient mice. Unexpectedly, neutrophilic chemokine KC expression was elevated in the lungs, especially in the BALF of IL-33-deficient mice treated with HDM and LPS (Figure 6a). Accordingly, the numbers of neutrophils in the BALF of HDM/LPS-coexposed IL-33-deficient mice were significantly increased (Figure 6b). In contrast, eosinophilic counts were increased slightly without statistical significance (Figure 6b). In addition, lung histological analysis revealed aggravated pulmonary inflammation in IL-33-deficient mice compared with their WT counterparts (Figure 6c).

We next examined whether lung epithelial barrier function was further deteriorated in IL-33-deficient mice. IL-33-deficient mice sensitised with HDM and LPS displayed increased lung epithelial permeability, as shown by the higher total protein contents in the BALF (Figure 6d). Similarly, further reduced expression of occludin was observed in the lungs of IL-33-deficient mice by immunohistochemistry analysis (Figure 6e). In contrast, the expression of MMP-9, known to damage the airway epithelial barrier, was elevated in IL-33-deficient treated mice (Figure 6f). Overall, our findings indicated that IL-33 deficiency may accentuate pulmonary inflammation in the development of neutrophil-dominant allergic airway disease, accompanied by worse epithelial barrier function.

ST2 deficiency augmented lung neutrophilic inflammation and tight junction damage in a murine model of neutrophil-dominant allergic airway disease

Although IL-33 generally exerts its cytokine activity by combining with its receptor ST2, several studies have revealed that the full-length form of IL-33 located in the nucleus may function in an ST2-independent manner.[32] To further decipher the role of the IL-33/ST2 axis in neutrophil-dominant allergic airway disease, we developed a murine model of neutrophil-dominant allergic airway inflammation in WT and ST2-deficient mice. We found that ST2 deficiency increased airway hyperresponsiveness and total serum IgE in the present neutrophil-

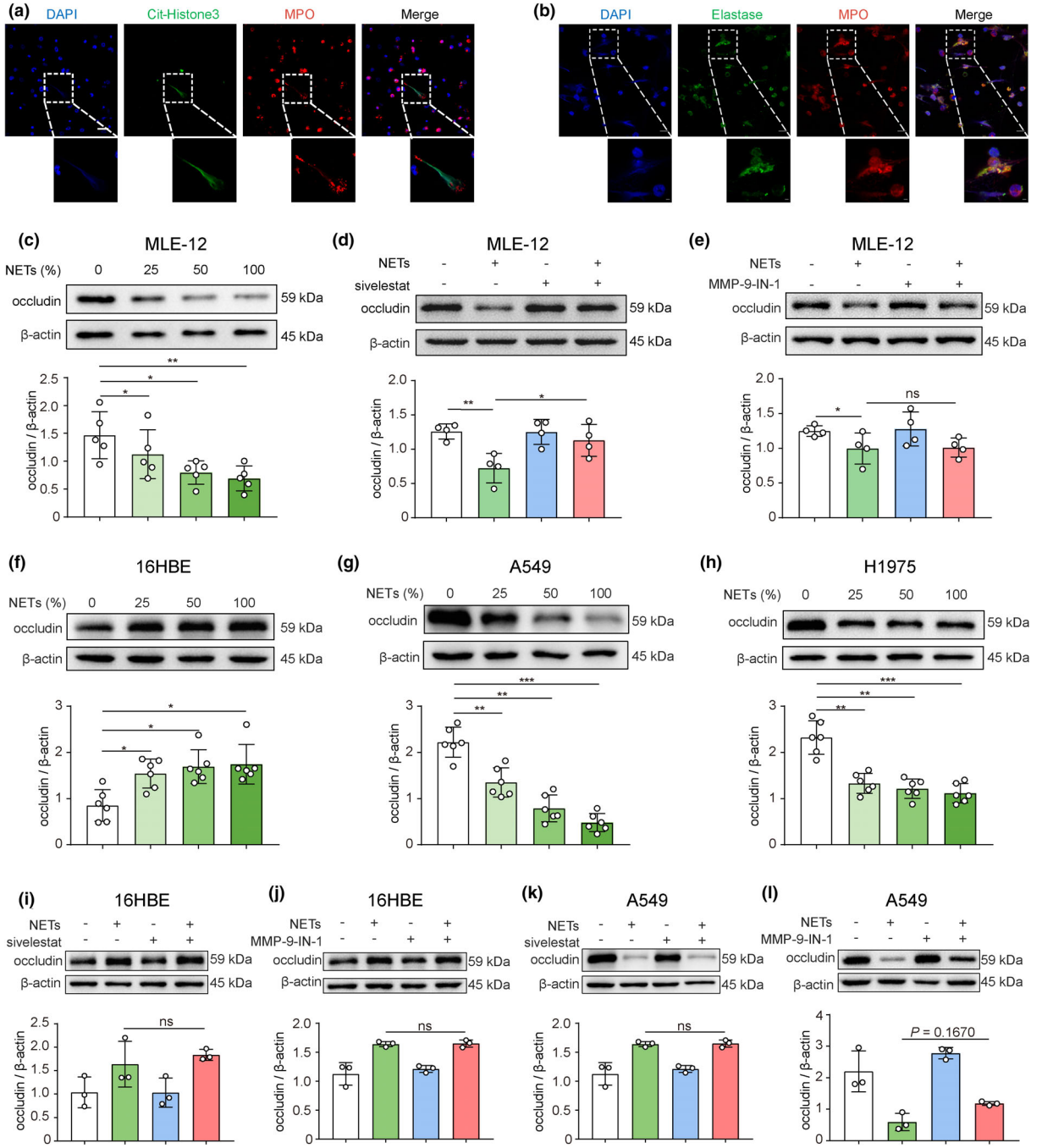

Figure 5. LPS damaged the tight junctions of lung epithelial cells indirectly by inducing NET formation. **(a, b)** NETs induced by LPS (1 μg mL^{-1}) *in vitro* were detected by immunofluorescence and identified as costained (dotted box) with DAPI (blue), **(a)** Cit-Histone3 (green) or **(b)** elastase (green) and MPO (red) (n = 3); original magnification 630× (top); scale bar, 10 μm; zoomed in 4× (bottom). **(c)** Occludin expression in MLE-12 cells cultured with various proportions of NET-rich media was analysed by Western blotting (n = 5). **(d, e)** Inhibition assays were performed using the inhibitor of **(d)** elastase (sivelestat, 500 nM)- or **(e)** MMP-9 (MMP-9-IN-1, 50 μM)-pretreated NET-rich media, and occludin expression was determined by Western blotting (n = 4). **(f–h)** Occludin expression in **(f)** 16HBE, **(g)** A549 or **(h)** H1975 cells cultured with various proportions of NET-rich media was analysed by Western blotting (n = 6). **(i, j)** 16HBE cells were stimulated with inhibitor of **(i)** elastase (sivelestat, 500 nM)- or **(j)** MMP-9 (MMP-9-IN-1, 50 μM)-pretreated NET-rich media, and occludin expression in cells was determined by Western blotting (n = 3). **(k, l)** A549 cells were stimulated with the inhibitor of **(k)** elastase (sivelestat, 500 nM)- or **(l)** MMP-9 (MMP-9-IN-1, 50 μM)-pretreated NET-rich media, and occludin expression in cells was determined by Western blotting (n = 3). Bar graphs and data are presented as the mean ± SD. *P < 0.05, **P < 0.01 and ***P < 0.001. ns, not significant.

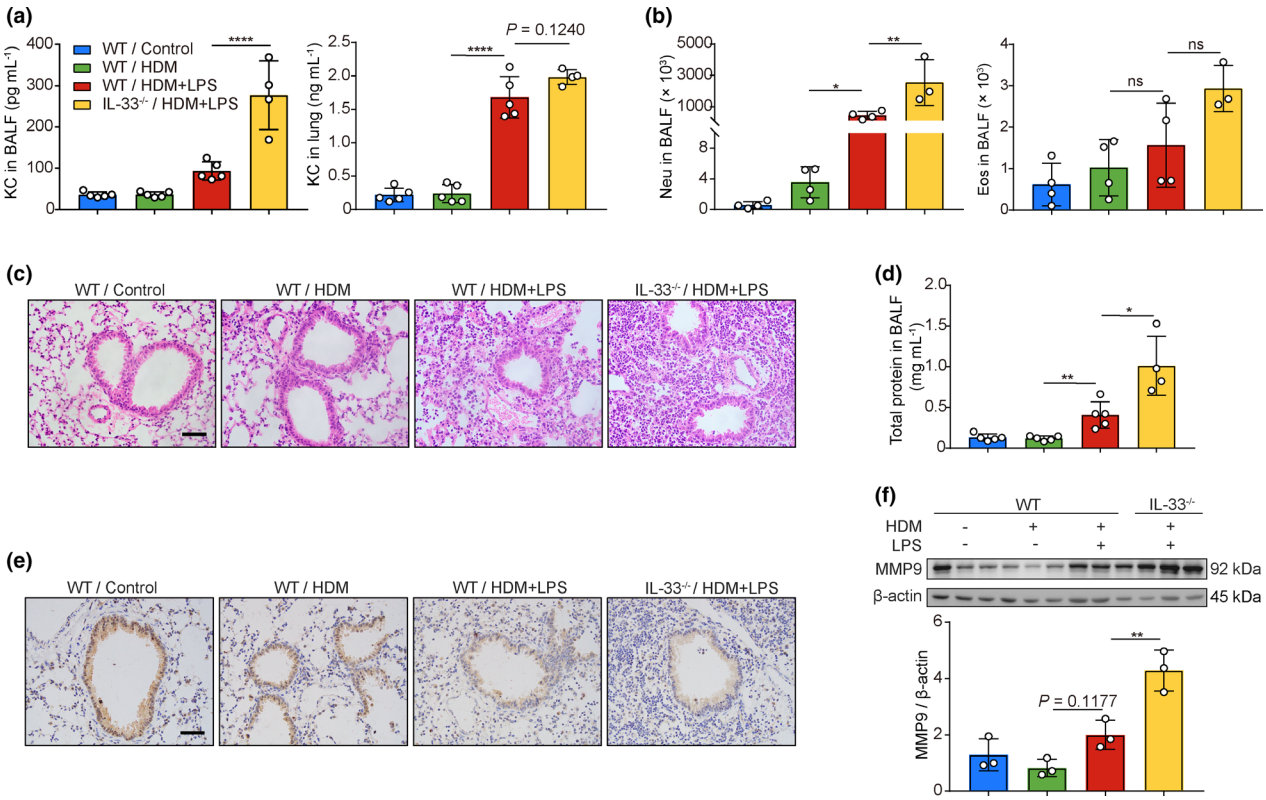

Figure 6. IL-33 deficiency aggravated airway neutrophilic inflammation and promoted lung epithelial barrier injury during allergen sensitisation. Wild-type (WT) mice were treated with HDM/LPS, HDM or PBS, and IL-33-deficient (IL-33$^{-/-}$) mice were sensitised with HDM/LPS. Mice were sacrificed at day 3. Shown are representative results from 2 independent experiments with 3, 4 or 5 mice per group. **(a)** KC contents in the BALF and lung were determined by ELISA. **(b)** Numbers of neutrophils (Neu) and eosinophils (Eos) in the BALF were measured by flow cytometry. **(c)** Representative images of histological lung sections stained with H&E for evaluating infiltration of inflammatory cells. **(d)** Total protein contents in BALF were determined by the Bradford protein assay for analysis of lung epithelial barrier injury. **(e)** Representative images of immunohistochemical staining for occludin expression in the lung. **(f)** The expression of MMP-9 in the lung was determined by Western blotting. Original magnification 400×; scale bar, 50 μm. Bar graphs and data are presented as the the mean ± SD. *$P < 0.05$, **$P < 0.01$ and ****$P < 0.0001$. ns, not significant.

dominant allergic airway inflammation (Figure 7a and b). Furthermore, the production of the chemokine KC was elevated in both the BALF and the lungs of ST2-deficient mice (Figure 7c). In addition, ST2 deficiency aggravated the inflammatory response in the lungs, as shown by histological analysis, consistent with the impact of IL-33 deficiency during sensitisation, whereas goblet cell hyperplasia and mucus secretion were comparable between HDM/LPS-treated WT and ST2-deficient mice (Figure 7d). Moreover, occludin expression was reduced, accompanied by increased MMP-9 expression in the lungs of ST2-deficient mice (Figure 7e). In summary, these results implied that IL-33/ST2 axis deficiency had a harmful impact on lung inflammation and the epithelial barrier.

IL-33/ST2 axis deficiency promoted neutrophilic infiltration via upregulated KC and CXCR2

Herein, we demonstrated that the absence of IL-33 or ST2 augmented neutrophilic inflammation accompanied by the elevation of chemokine KC expression in the BALF and lungs of mice treated with HDM and LPS. KC is reportedly expressed by macrophages and epithelial cells.[33] Therefore, we explored whether the expression of KC in bone marrow-derived macrophages (BMDMs) from WT and IL-33- or ST2-deficient mice was different. Interestingly, BMDMs from IL-33- or ST2-deficient mice displayed higher levels of KC mRNA and protein expression (Figure 8a). Primary alveolar epithelial cells isolated from the lungs were

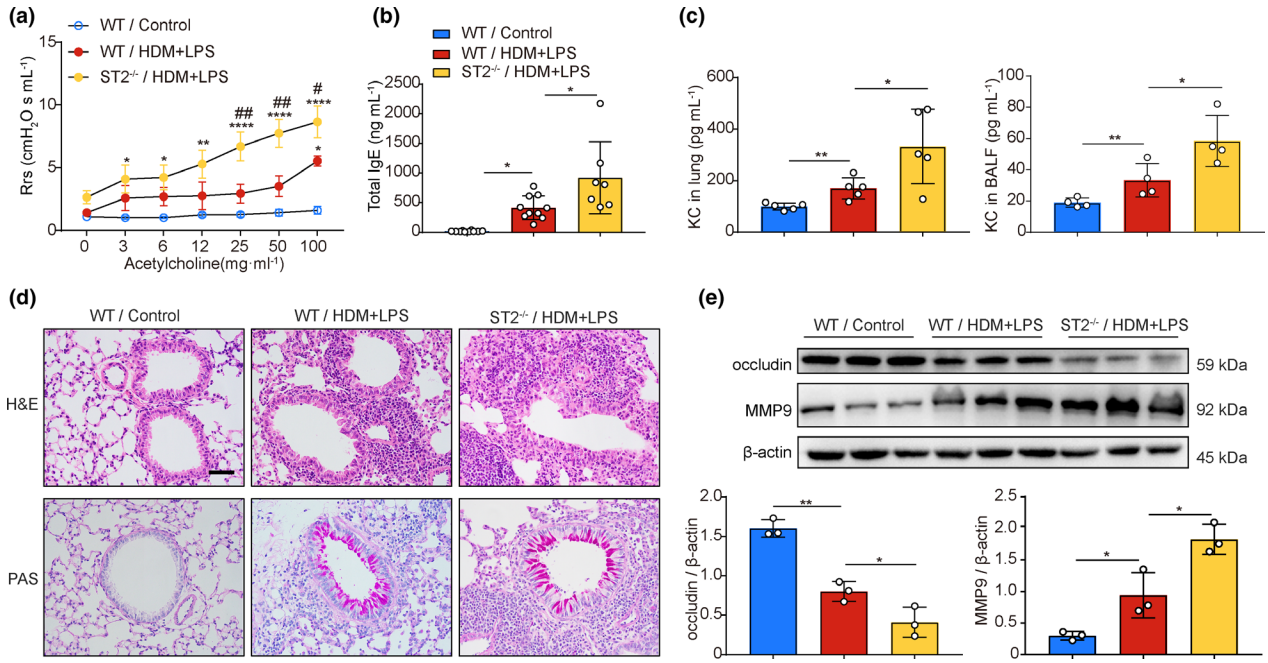

Figure 7. ST2 deficiency augmented lung neutrophilic inflammation and tight junction damage in a murine model of neutrophil-dominant allergic airway disease. WT and ST2-deficient ($ST2^{-/-}$) mice were sensitised with HDM/LPS and challenged with HDM, and WT mice were treated with PBS during both sensitisation and challenge as a control group. Shown are representative results from 2 independent experiments with 3, 4, 5, 7 or 10 mice per group. **(a)** Resistance of the respiratory system (Rrs) was measured in the presence of ascending doses of inhaled acetylcholine. **(b)** The level of total IgE in the serum was measured by ELISA. **(c)** KC contents in the BALF and lung were determined by ELISA. **(d)** Representative images of histological lung sections stained with H&E for evaluating infiltration of inflammatory cells and with PAS to analyse goblet cell hyperplasia; original magnification 400×; scale bar, 50 μm. **(e)** The expression levels of occludin and MMP-9 were determined by Western blotting. Bar graphs and data are presented as the mean ± SD. $^{*}P < 0.05$, $^{**}P < 0.01$ and $^{****}P < 0.0001$ *vs* WT/control; $^{\#}P < 0.05$, $^{\#\#}P < 0.01$ *vs* WT/HDM+LPS.

proven to be of high purity (Figure 8b). Similarly, the protein level of KC in the supernatant of cultured IL-33- or ST2-deficient alveolar epithelial cells and the mRNA level in cells were higher than those of their WT counterparts (Figure 8c). To further validate the findings, IL-33 expression in 16HBE cells was silenced with a CRISPR/Cas9/sgRNA complex plasmid. Accompanied by IL-33 reduction (Figure 8d), the mRNA level of neutrophilic chemokine CXCL1 (also known as KC in mice) was upregulated (Figure 8e). It has been reported that CXCL1 can be regulated by NF-κB.[34] To elucidate the molecular mechanism of KC upregulation in IL-33/ST2 axis-deficient cells, the activation level of NF-κB was analysed. However, there were no differences in the level of p-NF-κB in BMDMs (Figure 8f) or the nuclear translocation of NF-κB in primary alveolar epithelial cells (Figure 8g) between the WT and IL-33/ST2 axis-deficient groups. Since the IL-33/ST2 axis may regulate neutrophilic chemotaxis by regulating C-X-C chemokine receptor type 2 (CXCR2) on the surface of neutrophils,[35] we next analysed CXCR2 expression on both peripheral blood and BALF neutrophils of mice that were exposed to LPS for 24 h. The frequencies of CXCR2 expression on blood neutrophils and the mean fluorescence intensity (MFI) of CXCR2 on BALF neutrophils were upregulated in IL-33-deficient mice (Supplementary figure 1, Figure 8h and i). Additionally, CXCR2 expression on ST2-deficient neutrophils tended to rise, although the difference was not statistically significant (Figure 8h and i). These findings suggested that IL-33/ST2 axis deficiency might augment neutrophilia *in vivo* by upregulating KC secretion from macrophages and epithelial cells and CXCR2 expression on neutrophils.

DISCUSSION

Allergic asthma is a chronic respiratory disease with marked airway inflammation heterogeneity, and neutrophilic airway inflammation presents in

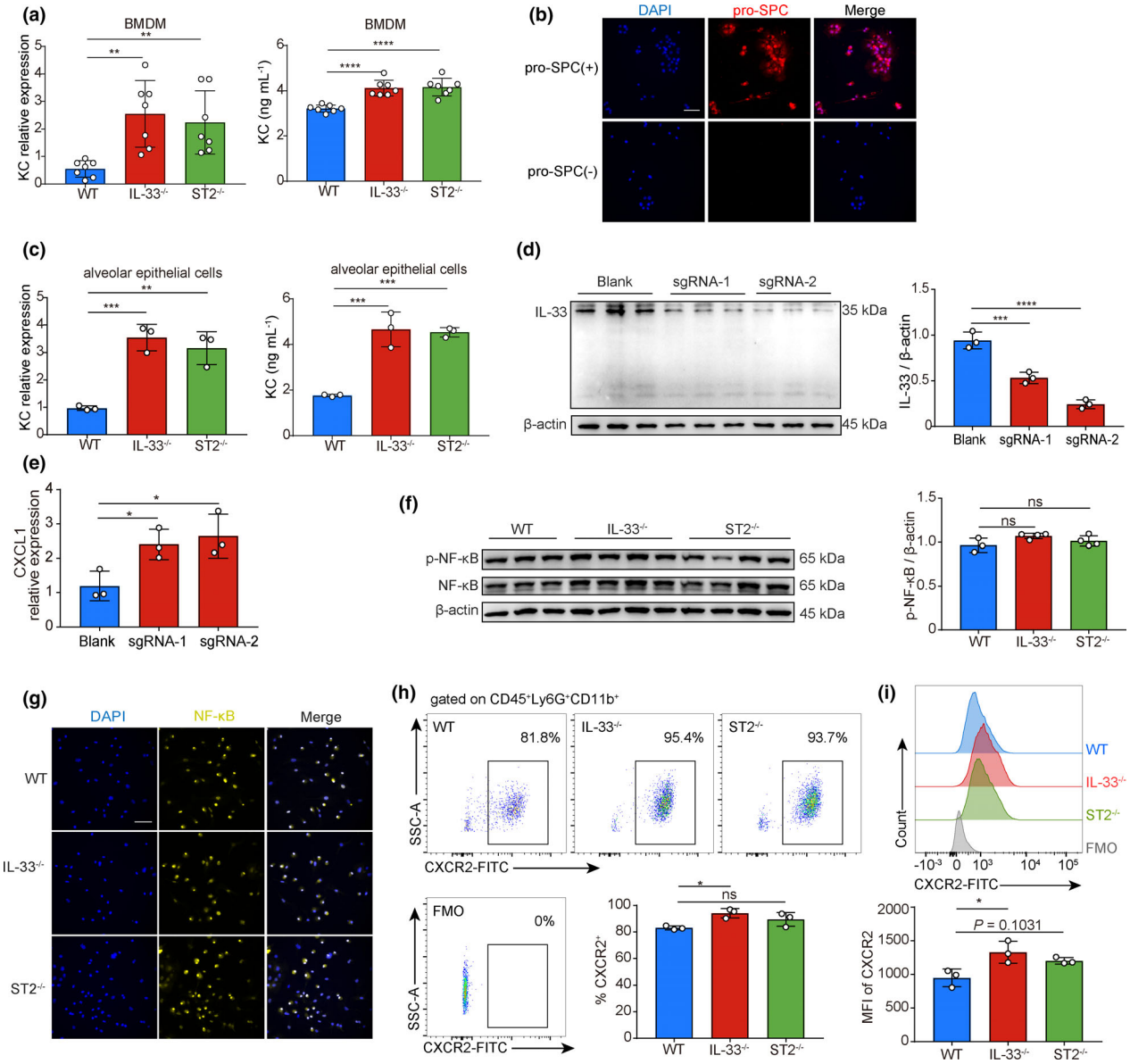

Figure 8. IL-33- or ST2-deficient BMDMs and lung epithelial cells were more proinflammatory. Shown are representative results from two independent experiments with 3 or 7 mice per group. **(a)** BMDMs were cultured from WT and IL-33-deficient ($IL\text{-}33^{-/-}$) or ST2-deficient ($ST2^{-/-}$) mice. KC mRNA levels in cells and protein levels in their culture supernatant were measured by qPCR and ELISA respectively. **(b)** Expression of pro-SPC on isolated primary alveolar epithelial cells was determined by immunofluorescence to assess the purity of the cells; original magnification 400× (top); scale bar, 50 μm. **(c)** Primary alveolar epithelial cells were isolated and cultured from WT and $IL\text{-}33^{-/-}$ or $ST2^{-/-}$ mice. KC mRNA levels in cells and protein levels in their culture supernatant were measured by qPCR and ELISA respectively. **(d, e)** 16HBE cells were transfected with human IL-33 sgRNA CRISPR/Cas9 All-in-One Lentivector or blank vector plasmids for 72 h. **(d)** The protein level of IL-33 in transfected 16HBE cells was analysed by Western blotting, **(e)** and the mRNA level of CXCL1, known as KC in mice, was detected by qPCR (n = 3/group). **(f)** Expression of p-NF-κB and NF-κB was determined by Western blotting in untreated BMDMs from WT, $IL\text{-}33^{-/-}$ and $ST2^{-/-}$ mice. **(g)** The expression and location of NF-κB were analysed by immunofluorescence in untreated WT, $IL\text{-}33^{-/-}$ and $ST2^{-/-}$ primary alveolar epithelial cells. **(h, i)** Blood and BALF cells were collected after the mice were intratracheally treated with 10 μg LPS for 24 h. **(h)** Frequencies of CXCR2 expression in circulating neutrophils **(i)** and mean fluorescence intensity (MFI) of CXCR2 expression in BALF neutrophils were analysed by flow cytometry. Bar graphs and data are presented as the mean ± SD. $^{*}P < 0.05$, $^{**}P < 0.01$, $^{***}P < 0.001$ and $^{****}P < 0.0001$. ns, not significant.

approximately 50% of patients with severe asthma.[1,2] Recently, evidence emerged indicating that the IL-33/ST2 axis, which has largely been studied in the setting of eosinophilic and type 2 asthma, may inhibit neutrophilic inflammation in some contexts.[36,37] However, the role of the IL-33/ST2 axis in neutrophil-dominant allergic airway inflammation remains elusive. Here, we showed that airway exposure to HDM and LPS promoted the pulmonary neutrophilic inflammatory response and damaged epithelial barrier function. Moreover, these alterations occurred as early as the sensitisation period alongside increased NET formation and IL-33 maturation. Of importance, IL-33/ST2 deficiency amplified neutrophilic inflammation and epithelial barrier injury and further augmented the severity of neutrophil-dominant allergic airway inflammation characterised by elevated airway hyperresponsiveness and higher total IgE levels.

Once the integrity of barrier function is damaged, more inhaled allergens or other environmental pollutants may be allowed to penetrate the epithelium. Several documents have revealed tight junction disorders in asthmatic airways.[9,10,12,13] Accordingly, we observed the presence of epithelial barrier injury characterised by decreased occludin expression in the HDM/LPS-induced allergic airway disease model, along with dramatically increased total IgE associated with the severity of allergic airway inflammation. Similarly, occludin expression was further decreased in HDM/LPS-treated ST2-deficient mice, accompanied by increased airway hyperresponsiveness and even higher total IgE levels. Therefore, the epithelial barrier injury present in asthmatic airways may be associated with the severity of asthma.

Neutrophilic extracellular traps have recently been associated with severe asthma, as reported that NET components could be detected in a subset of severe asthma cases and are related to the severity of disease.[7,38] Given that neutrophilic proteases (such as neutrophilic elastase and MMP-9) decorated on NETs can degrade tight junction proteins,[39] NETs may be implicated in severe asthma pathogenesis by disrupting lung epithelial tight junctions. Accordingly, we observed that NETs were increased in the lungs of mice sensitised with HDM and LPS in the present study. Moreover, occludin expression on lung epithelial cells was decreased by NETs *in vitro* and restored by inhibiting the activity of elastase instead of MMP-9. However, MMP-9 was reported to modulate tight junction integrity in human airway epithelial cells.[39] Additionally, our *in vivo* experiments showed that MMP-9 expression was significantly upregulated in the HDM/LPS-treated groups. One plausible explanation is that NETs induced *in vitro* by LPS alone might not contain much MMP-9, and increased MMP-9 expression *in vivo* is mainly related to enhanced neutrophilic inflammation.

IL-33 has been reported to function as a pleiotropic cytokine involved in immune regulation, host defence, tissue repair and metabolic homeostasis.[40] IL-33/ST2 signalling plays a vital role in asthma, especially in the setting of a type 2 inflammatory response.[41] Briefly, IL-33 stimulates type 2 innate lymphoid cells (ILC2s) or Th2 cells to produce type 2 cytokines, leading to lung eosinophilic inflammation. Recently, an increasing number of studies have suggested that the IL-33/ST2 axis regulates the pulmonary neutrophilic inflammatory response. For instance, ST2-deficient mice displayed enhanced inflammatory cell recruitment, primarily by neutrophils, 24 h after bleomycin treatment. Similarly, the absence of IL-33/ST2 signalling augmented neutrophilic inflammation and lung barrier injury in an ozone-exposed lung injury model.[36] Furthermore, a prospective observational study revealed that serum sST2 (a decoy receptor for IL-33 that inhibits IL-33/ST2 signalling) levels were positively correlated with asthma severity and could predict severe asthma exacerbation.[22] In line with these findings, we observed enhanced pulmonary neutrophilia and epithelial injury in IL-33- or ST2-deficient mice after HDM and LPS exposure. In addition, our study showed that the absence of ST2 elevated serum IgE levels and airway hyperresponsiveness in an HDM/LPS-induced neutrophil-dominant allergic airway disease model. Notably, mucus secretion was comparable between HDM/LPS-exposed WT and ST2-deficient mice. This may be explained by the fact that downregulation of IL-13 (a mucus secretion mediator[42]) by ST2 deficiency may offset the effect of more severe disease. Therefore, the IL-33/ST2 axis may play a protective role in neutrophil-dominant allergic airway inflammation. IL-33 is currently being investigated as a potential therapeutic target in a phase 2 clinical trial (ClinicalTrials.gov Identifier: NCT03112577). On the one hand, our data indicated that treatments targeting IL-33 may not lead to better clinical

outcomes in regard to treating neutrophilic asthma. On the other hand, treatments that target airway neutrophilia may be of no help to treat neutrophilic asthma. Neutrophilic depletion reportedly augmented type 2 allergic airway inflammation in an HDM-induced murine model of allergic airway disease.[43] Consistently, treatment with a selective CXCR2 antagonist did not reduce the occurrence of severe exacerbations in severe asthmatic patients.[44]

The mechanisms by which the IL-33/ST2 axis participates in regulating neutrophilic inflammation are largely unresolved. One possibility is that IL-33/ST2 axis may influence neutrophilic chemotaxis by regulating chemokine receptor CXCR2 expression on the surface of neutrophils.[35] ST2 negatively regulates IL-1 receptor (IL-1RI) and Toll-like receptor (TLR) signalling,[45] and CXCR2 can be downregulated by TLR engagement.[46] Furthermore, IL-33/ST2 axis may perform protective functions in neutrophilia by modulating macrophages. As previously described, BMDMs from IL-33-deficient mice are more proinflammatory after stimulation with LPS/IFN-γ, which induces type 1 macrophage skewing.[47] In the present study, we found that neutrophilic chemokine KC expression was higher in BMDMs and alveolar epithelial cells in the absence of IL-33 or ST2. Collectively, although the exact mechanisms by which the IL-33/ST2 axis regulates the neutrophilic inflammatory response are still unclear, they may partially be explained by the fact that IL-33/ST2 deficiency leads to a proinflammatory status in macrophages and epithelial cells.

In summary, we demonstrated that the IL-33/ST2 axis may play a protective function in the context of neutrophil-dominant allergic airway inflammation. LPS exposure during allergen sensitisation caused pulmonary neutrophilic inflammation and epithelial barrier injury directly or via the induction of NETs (Supplementary figure 2). The role of the IL-33/ST2 axis in asthma and other allergic airway inflammation disorders warrants further research.

METHODS

Mice and ethics statement

Wild-type female C57BL/6J mice aged 6–8 weeks were purchased from the Laboratory Animal Center, Nanjing Medical University (Nanjing, China) and Charles River Laboratories. IL-33-deficient and ST2-deficient mice with a C57BL/6J background were obtained as a gift from Dr Hong Zhou's Laboratory (Department of Immunology, Nanjing Medical University). Mice used for all experiments were bred under specific pathogen-free conditions at Nanjing Medical University. All animal protocols were reviewed and approved by the Animal Care and Use Committee of Nanjing Medical University (1709011).

Animal models

All reagents were administered via oropharyngeal aspiration (OPA) while mice were under isoflurane anaesthesia. For the house dust mite (HDM) and lipopolysaccharide (LPS)-induced neutrophil-dominant allergic airway disease model, 25 μg of HDM (Greer Laboratories, Lenoir, NC, USA) with 10 μg of LPS (L4391, *Escherichia coli* 0111:B4, Sigma-Aldrich, St. Louis, MO, USA) dissolved in 35 μL of sterile phosphate-buffered saline (PBS) was introduced into airways once daily for 3 days (days 0–2) during allergen sensitisation, and 25 μg of HDM alone in a volume of 35 μL was given to common asthma model mice. Four days later, the mice were challenged with 25 μg of HDM alone in 35 μL of sterile PBS once daily for 8 days (days 7–14). For the vehicle control group, the mice were treated with PBS throughout the process. Twenty-four hours after the last challenge (day 15), the mice were euthanised, serum and bronchoalveolar lavage fluid (BALF) was collected, and lung tissue was harvested for analysis. The protocol was deduced from existing HDM/LPS-induced allergic airway disease model.[26] In some experiments, the mice were sacrificed on day 3 to investigate pulmonary inflammation and epithelial barrier function during allergen sensitisation.

Airway responsiveness analysis

Mice were anaesthetised by intraperitoneal injection of sodium pentobarbital 24 h after the final challenge, and airway responsiveness was measured using a FlexiVent Pulmonary System (SCIREQ, Montreal, QC, Canada). Briefly, anaesthetised mice were mechanically ventilated and then challenged with incremental doses of aerosolised acetylcholine (0, 3.125, 6.25, 12.5, 25, 50 and 100 mg mL^{-1}, Sigma). Lung resistance was recorded for 2 min after each challenge.

Bronchoalveolar lavage fluid and serum collection

The mice were sacrificed by intraperitoneal injection of sodium pentobarbital. Subsequently, whole blood was collected, and serum was obtained by centrifuging blood (1200 *g*, 10 min) after clotting. BALF was obtained by an intratracheal injection of 0.5 $\times$ 3 mL of PBS containing 1 mM EDTA followed by gentle aspiration. BALF was centrifuged (500 *g*, 5 min). Cell-free supernatants were collected to determine the total protein concentrations and to perform cytokine analysis. Cell pellets were resuspended for cell counts by flow cytometry. Briefly, neutrophils ($CD45^+$ $Ly6G^+$ $F4/80^-$) and eosinophils ($CD45^+$ $SiglecF^+$ $F4/80^-$) were counted by counting beads (01-1234-42, eBioscience, San Diego, CA, USA) after staining with Fixable Viability Dye eFluor™ 506 (65-0866-14, eBioscience) and

blocking Fc receptor (FcR) with CD16/CD32 antibody (14-0161-85, eBioscience).

Bronchoalveolar epithelial permeability measurements

An increase in protein concentration in the BALF can reflect an increase in capillary leakage. Cell-free supernatants of BALFs were collected to measure lung epithelial barrier injury by detecting the total protein concentrations using the Bradford Protein Assay Kit (P0006, Beyotime, Shanghai, China).

In some experiments, bronchoalveolar epithelial permeability was determined by measuring the leakage of fluorescein isothiocyanate–dextran 4000 (FD4) from the airways into the blood. In short, 24 h after the last exposure, 20 μL of FD4 (25 mg mL^{-1}; 60842-46-8, Sigma-Aldrich) solution was instilled intratracheally into the airways of mice. Then, blood was collected 1 h after injection, and the fluorescence intensity of FD4 in the serum was measured using a fluorescence plate reader (BioTek Synergy, Winooski, VT, USA) at an excitation wavelength of 485 nm and an emission wavelength of 525 nm.

Lung histological analysis

After bronchoalveolar lavage was performed, PBS was pumped into the right ventricle to clear the blood in the pulmonary vasculature. Then, the left lung lobes were fixed in 4% paraformaldehyde (G1101, Servicebio, Wuhan, China) before dehydration and paraffin embedding. Subsequently, lung tissues were cut into 5-μm-thick sections and stained with haematoxylin and eosin (H&E) or periodic acid–Schiff (PAS) to estimate the extent of inflammation or mucus production. Sections were captured at a magnification of 400× with a microscope (model BX-53, Olympus Optical, Tokyo, Japan) by an investigator blinded to the groups.

Immunohistochemistry

Pulmonary sections (5 μm) were cut from paraffin-embedded lung tissue, followed by deparaffinisation and antigen retrieval. Next, 3% H_2O_2 solution was used to inhibit endogenous peroxidase activity, and 10% goat serum was applied to block nonspecific binding. Tissue sections were then incubated with anti-occludin antibody (1:200; ab216327, Abcam, Cambridge, UK) overnight at 4 °C, followed by incubation with horseradish peroxidase (HRP)-conjugated goat anti-rabbit IgG (1:1000; EarthOx, Millbrae, CA, USA) for 1 h at room temperature. Finally, colour development was immediately performed using 3,3-diaminobenzidine (DAB), followed by haematoxylin counterstaining.

Immunofluorescence staining

For NET staining *in vivo* experiments, lung tissue sections were prepared as described above. After deparaffination and antigen retrieval, sections were blocked with 10% goat serum for 30 min at 37 °C and incubated with the following primary antibodies overnight at 4 °C: anti-citrullinated histone 3 (1:200; ab5103, Abcam) and anti-myeloperoxidase (1:50; ab90810, Abcam). After three washes, the sections were stained with Alexa Fluor 555 goat anti-rabbit IgG (H + L) (1:500; A21428, Invitrogen, Waltham, Massachusetts, USA) and Alexa Fluor 647 goat anti-mouse IgG (H + L) (1:1000; A21235, Invitrogen) secondary antibodies for 1 h at 37 °C in the dark. Finally, 4′,6-diamidino-2-phenylindole (DAPI; 36308ES20, Yeasen, Shanghai, China) was applied to stain the DNA. To identify NETs induced *in vitro*, NETs were stained consistent with *in vivo* experiments, and anti-citrullinated histone 3 was replaced by anti-elastase (1:100; ab21595, Abcam) in some experiments. To verify the purity of isolated alveolar epithelial cells, anti-pro-SPC (1:250; ab170699, Abcam) primary antibody accompanied by Alexa Fluor 555 goat anti-rabbit IgG (H + L) (1:500; A21428, Invitrogen) secondary antibody was used to mark type 2 alveolar epithelial cells. The primary antibody anti-NF-κB (1:400; 8242S, Cell Signaling Technology, Danvers, MA, USA) was used to analyse the expression and location of NF-κB in primary alveolar epithelial cells. Slides were visualised with a ZEISS LSM710 confocal fluorescence microscope or an Olympus IX73 fluorescence microscope.

Enzyme-linked immunosorbent assay

Enzyme-linked immunosorbent assay (ELISA) was performed according to the manufacturer's instructions provided by commercially available ELISA kits. Levels of total immunoglobulin E (IgE) in the serum were determined by an ELISA kit (432404, BioLegend, San Diego, CA, USA), and cytokine concentrations in the supernatants of lung homogenates, BALF or cell culture supernatants were measured with appropriate ELISA kits as follows: KC (DY453-05, R&D, Minneapolis, MN, USA), MCP-1 (887324, BioLegend; DY453-05, R&D), eotaxin (DY420-05, R&D), IL-1β (88-7013-88, Invitrogen), TNF-α (88-7324-88, Invitrogen), IL-6 (88-7064-88, Invitrogen), IL-13 (900-K207, PeproTech, Rocky Hill, CT, USA) and IL-33 (88-7333-88, Invitrogen; DY3626, R&D).

The level of HDM-specific IgE (HDM-IgE) was measured by sandwich ELISA. Briefly, 96-well ELISA plates were coated with rabbit anti-Dust Mite Der P1 monoclonal antibody (CABT-L017, Creative Diagnostics, New York, USA) in 100 μL PBS (1:500) and incubated overnight at 4 °C. Plates were incubated with 2 μg HDM in 100 μL PBS for 2 h at room temperature. Plates were blocked with 200 μL per well of assay diluent. A 100 μL aliquot of diluent (1:10) serum samples was added to each well and incubated for 2 h. HRP-goat anti-mouse IgE secondary antibody (PA1-84764, Invitrogen) in 100 μL assay diluent (1:500) was added and incubated for 30 min. TMB substrate solution was added and incubated in the dark for 25 min, and the reaction was stopped with ELISA Stopping Solution (C1058, Solarbio, Beijing, China). Optical densities (ODs) were read at 450 nm with reference at 570 nm.

Isolation of neutrophils

Mouse neutrophils were isolated from bone marrow by density gradient centrifugation as previously described.[48] The mice were euthanised and immersed in 75% ethanol for 10 min. Tibias and femurs were separated from both

legs by blunt dissection and then rinsed three times with sterile PBS. Bone marrow cells were flushed with PBS and filtered through a 70-μm filter. The collected cell suspension was centrifuged (500 *g*, 5 min, 4 °C) and resuspended in 1 mL cold sterile PBS. Then, separation media and suspension were gently added into a 15-mL conical tube in accordance with the following order: 3 mL of Histopaque 1119 (density 1.119 g mL^{-1}; 11191, Sigma-Aldrich), 3 mL of Histopaque 1077 (density 1.077 g mL^{-1}; 10771, Sigma-Aldrich) and 1 mL of bone marrow cell suspension. Finally, neutrophils at the interface of the Histopaque 1119 and Histopaque 1077 layers were obtained after centrifugation (800 *g*, 30 min, 25 °C) without braking. The purity and viability of isolated neutrophils were verified by Wright–Giemsa staining and trypan blue assay respectively.

Human neutrophils were isolated from fresh human whole blood by a human peripheral blood neutrophil separation solution kit (P9040, Solarbio) according to the manufacturer's instructions. Human whole blood was collected from healthy donors under approval by the ethics committee of the First Affiliated Hospital of Nanjing Medical University (2017-SR-087).

NET generation and collection

After isolation, neutrophils (1×10^6 mL^{-1}) were seeded and allowed to adhere to culture plates in serum-free RPMI 1640 culture media for 1 h. Then, the cells were incubated with either LPS (1 μg mL^{-1}, Sigma-Aldrich) or phorbol 12-myristate 13-acetate (PMA, 500 nM; Sigma-Aldrich) for 4 h to induce NET formation. For NET collection, the culture media were gently discarded, and the plates were washed three times with PBS. Subsequently, 10 mL of DMEM/F12 supplemented with 10% foetal bovine serum (FBS; Lonsera, Shanghai, China) and 100 IU mL^{-1} penicillin/streptomycin (HyClone, Marlborough, USA) were added to the plate and then collected in a 15-mL conical tube after vigorous agitation. NET-rich media were obtained by centrifugation (500 *g*, 5 min, 4 °C) to remove neutrophils and cellular debris.

Cell stimulation and inhibitor assays

Mouse lung epithelial cells (MLE-12), human lung cancer cells (A549), human lung adenocarcinoma cells (H1975) and human bronchial epithelial cells (16HBE) were purchased from ATCC (Manassas, VA, USA). All these cells were cultured in DMEM/F12 media supplemented with 10% FBS and 100 IU mL^{-1} penicillin/streptomycin in 5% CO_2 at 37 °C. To study the direct effect of LPS on the lung epithelial barrier, MLE-12 and 16HBE cells were treated with various concentrations of LPS (0, 0.1, 1, or 10 μg mL^{-1}) for 24 h. For inhibition assays, MLE-12 and 16HBE cells were pretreated with an inhibitor of NF-κB (BAY 11-7082, 10 μM; S2913, Selleckchem, Shanghai, China) 1 h before LPS stimulation. When investigating the impact of NETs on epithelial tight junctions, MLE-12 cells and 16HBE, A549 and H1975 cells were stimulated with different proportions of mouse NET-rich or human NET-rich media (0%, 25%, 50% and 100%) for 24 h. For inhibition assays, NET-rich media were pretreated with either a selective inhibitor of neutrophilic elastase (sivelestat, 500 nM; 324759, Millipore, Burlington, MA, USA) or a specific MMP-9 inhibitor (MMP-9-IN-1, 50 μM; HY-135232, MCE, Shanghai, China) for 1 h at 37 °C before stimulating MLE-12 cells.

Bone marrow-derived macrophage culture

Bone marrow cells obtained as above were seeded in 24-well cell culture plates (1×10^6 cells per well) with 0.5 mL of complete DMEM containing 20 ng mL^{-1} GM-CSF (576306, BioLegend), 10% FBS and 100 IU mL^{-1} penicillin/streptomycin for 3 days. Subsequently, another 0.5 mL of fresh complete DMEM was added to each well and cultured for 3 days. The culture supernatants of BMDMs were replaced with 1 mL of fresh DMEM at day 6. Finally, cells and supernatants were collected after 24 h for cytokine analysis.

Primary alveolar epithelial cell isolation and culture

Primary alveolar epithelial cell isolation was performed as previously described.[49] The lungs of anaesthetised mice were inflated with 1 mL of digestion buffer (0.1% collagenase and 0.25% trypsin) after lung vasculature perfusion. Then, the lung lobes were digested for 45 min at room temperature, followed by digestion with supplementary DNase (5 mg mL^{-1}; DN25–1G, Sigma-Aldrich) for another 10 min. After filtration through a 40-μm filter, alveolar epithelial cells in suspension were purified by adherence to IgG-coated plates. The isolated alveolar epithelial cells were cultured on 24-well plates (1×10^6 cells per well) in DMEM/F12 media supplemented with 10% FBS and 100 IU mL^{-1} penicillin/streptomycin for 24 h to adhere. Subsequently, the culture media were refreshed, and the cells were cultured for another 24 h. Finally, alveolar epithelial cells and their culture supernatants were harvested for cytokine analysis.

Western blotting

Lung tissues were homogenised, and cells were dissociated with RIPA buffer (89901, Thermo Fisher, Waltham, MA, USA) containing phenylmethylsulphonyl fluoride (PMSF; ST506, Beyotime). The cell-free supernatants of lung homogenates, cell lysates and BALF were solubilised in sodium dodecyl sulphate–polyacrylamide gel electrophoresis (SDS-PAGE) protein loading buffer and boiled at 100 °C for 10 min. Equal amounts of proteins were separated on a 10–15% SDS-PAGE gel and transferred onto polyvinylidene fluoride (PVDF) membranes. Membranes were blocked with 5% skim milk (w/v) for 1 h at room temperature and subsequently incubated overnight at 4 °C with the following primary antibody in the universal antibody diluent (WB500D; NCM Biotech, Suzhou, China): anti-β-actin (1:1000; 4970L, Cell Signaling Technology), anti-occludin (1:1000; ab216327, Abcam), anti-claudin-3 (1:500; ab15102, Abcam), anti-claudin-4 (1:500; ab15104, Abcam), anti-IL-33 (1:1000; ab187060, Abcam), anti-human IL-33 (1:1000; ab207737, Abcam), anti-citrullinated histone 3 (1:1000; ab5103, Abcam), anti-MMP-9 (1:1000; ab76003, Abcam),

anti-p-NF-κB (1:1000; 3033S, Cell Signaling Technology) and anti-NF-κB (1:1000; 8242S, Cell Signaling Technology). Membranes were washed with Tris-buffered saline/Tween-20 (TBST) three times and then incubated with HRP-conjugated goat anti-rabbit IgG (EarthOx) for 1 h at room temperature. After washing three more times with TBST, the antibody–antigen complexes were detected with Immobilon Western Chemiluminescent HRP Substrate (36208ES76, Yeasen) and visualised using a G:Box gel doc system (Tanon 5200, Shanghai, China). The images were analysed using the ImageJ software. For proteins in lung tissues and cells, β-actin was used as the internal control. For proteins in BALF, Ponceau S was used as the loading control.

RNA isolation and quantitative real-time PCR

Total RNA was isolated from lung tissues and cells using a TRIzol reagent kit (15596018, Life Technologies, Carlsbad, CA, USA) according to the manufacturer's instructions. Then, mRNAs were reverse-transcribed into cDNA with a 5X All-In-One RT MasterMix Kit (G490, Abm, Zhenjiang, China). cDNAs were amplified using EvaGreen PCR Master Mix Applied Biosystems (MasterMix-S, Abm) and a StepOnePlus Real-Time PCR System (Applied Biosystems, Waltham, MA, USA). KC/CXCL1 and β-actin mRNA expressions were detected. The primer sequences for those genes were designed by referring to PrimerBank (https://pga.mgh.harvard.edu/primerbank). The primer sequences used were as follows:

Mouse β-actin forward, GAGAAGCTGTGCTATGTTGCT
Mouse β-actin reverse, CTCCAGGGAGGAAGAGGATG
Human β-actin forward, CATGTACGTTGCTATCCAGGC
Human β-actin reverse, CTCCTTAATGTCACGCACGAT
Mouse KC forward, ACTGCACCCAAACCGAAGTC
Mouse KC reverse, TGGGGACACCTTTTAGCATCTT
Human CXCL1 forward, AGCTTGCCTCAATCCTGCATCC
Human CXCL1 reverse, TCCTTCAGGAACAGCCACCAGT

Relative levels were determined using the comparative threshold cycle (ΔΔCT) method by normalising to β-actin.

Transfection

To silence IL-33 expression, 16HBE cells were transfected with human IL-33 sgRNA CRISPR/Cas9 All-in-One LentiVector (sgRNA-1 targeting sequences: GGAGCTTCATAAAGTACATG; sgRNA-2 targeting sequences: TACTTTATGAAGCTCCGCTC) and blank Control Lentiviral Vector plasmids (CS33781, Abm) using Liposomal Transfection Reagent (40802ES03, Yeasen) according to the manufacturer's instructions. Briefly, 16HBE cells were seeded and incubated overnight. The plasmids were mixed with Liposomal Transfection Reagent in DMEM/F12 for 20 min and were then transfected into 16HBE cells at 80% density in DMEM/F12 for 6 h. Then, the culture media were replaced with fresh completed DMEM/F12. Seventy-two hours later, cells were split for either analysing CXCL1 expression by qPCR or measuring the efficiency of targeting IL-33 by Western blotting.

CXCR2 expression analysis

For CXCR2 expression on the surface of neutrophilic analysis, 10 μg LPS was intratracheally induced into the airways of WT, IL-33$^{-/-}$ and ST2$^{-/-}$ mice. Twenty-four hours later, approximately 300 μL whole blood of LPS-treated mice was collected into sterile tubes containing 100 μL EDTA (15 g L^{-1}) and then incubated with 3 mL RBC lysis buffer (00-4333, Invitrogen) at 4 °C for 5 min. Subsequently, BALF was harvested as previously described. Both blood cells and BALF cells were washed with sterile PBS twice for flow cytometry analysis. Cells were stained with the fixable viability dye Zombie NIR (423105, BioLegend) for 15 min. Subsequently, cells were labelled with CD45-PE/Cy7 (103114, BioLegend), Ly6G-APC (108412, BioLegend), CD11b-BV510 (101263, BioLegend) and CXCR2-FITC (149310, BioLegend) after blocking the Fc receptor (FcR) with CD16/CD32 antibody (14-0161-85, eBioscience). CD45$^+$ Ly6G$^+$ CD11b$^+$ cells were identified as neutrophils.

Statistics

All statistics were calculated using the GraphPad Prism 7 (San Diego, CA, USA). The results are expressed as the mean ± SD. Statistical differences were calculated by the two-tailed unpaired Student's *t*-test between two groups and by parametric one-way analysis of variance (ANOVA) with Tukey's adjustment between multiple groups. Statistical significance was defined as follows: $^*P < 0.05$, $^{**}P < 0.01$, $^{***}P < 0.001$ and $^{****}P < 0.0001$. ns, not significant.

ACKNOWLEDGMENTS

This research was supported by the Precision Medicine Research of the National Key Research and Development Plan of China (2016YFC0905800), the National Natural Science Foundation of China (81671563, 81770031, 81700028 and 81970031), the Natural Science Foundation of Jiangsu Province (BK20171501, BK2017080 and BK20181497), Jiangsu Province's Young Medical Talent Program, China (QNRC2016600), and the Jiangsu Provincial Health and Family Planning Commission Foundation (Q2017001).

CONFLICT OF INTEREST

The authors declare no conflict of interest.

AUTHOR CONTRIBUTIONS

Qiyun Ma: Conceptualization; Data curation; Investigation; Methodology; Writing-original draft. **Yan Qian:** Formal analysis; Methodology; Writing-original draft. **Jingxian Jiang:** Methodology; Validation; Visualization. **Jingjing Wu:**

Data curation; Investigation; Methodology. **Meijuan Song:** Methodology; Validation. **Xinyu Li:** Methodology. **Zhongqi Chen:** Formal analysis; Validation. **Zhengxia Wang:** Formal analysis; Methodology; Validation. **Ranran Zhu:** Formal analysis; Methodology. **Zhixiao Sun:** Methodology; Validation. **Mao Huang:** Conceptualization; Funding acquisition; Supervision; Writing-review & editing. **Ningfei Ji:** Conceptualization; Funding acquisition; Project administration; Writing-review & editing. **Mingshun Zhang:** Conceptualization; Data curation; Funding acquisition; Project administration; Supervision; Writing-review & editing.

ETHICS APPROVAL AND CONSENT TO PARTICIPATE

All experiments that involved animal and tissue samples were performed in accordance with the guidelines and procedures approved by the Institutional Animal Care and Use Committee of Nanjing Medical University (IRB: 1709011).

DATA AVAILABILITY STATEMENT

The data sets used and/or analysed during the present study are available from the corresponding author upon reasonable request.

REFERENCES

1. Simpson JL, Scott R, Boyle MJ, Gibson PG. Inflammatory subtypes in asthma: assessment and identification using induced sputum. *Respirology* 2006; **11**: 54–61.
2. Green RH, Brightling CE, Woltmann G, Parker D, Wardlaw AJ, Pavord ID. Analysis of induced sputum in adults with asthma: identification of subgroup with isolated sputum neutrophilia and poor response to inhaled corticosteroids. *Thorax* 2002; **57**: 875–879.
3. Moore WC, Hastie AT, Li X *et al*. Sputum neutrophil counts are associated with more severe asthma phenotypes using cluster analysis. *J Allergy Clin Immunol* 2014; **133**: 1557–1563.e1555.
4. Brinkmann V, Reichard U, Goosmann C *et al*. Neutrophil extracellular traps kill bacteria. *Science* 2004; **303**: 1532–1535.
5. Kaplan MJ, Radic M. Neutrophil extracellular traps: double-edged swords of innate immunity. *J Immunol* 2012; **189**: 2689–2695.
6. Gál Z, Gézsi A, Pállinger É *et al*. Plasma neutrophil extracellular trap level is modified by disease severity and inhaled corticosteroids in chronic inflammatory lung diseases. *Sci Rep* 2020; **10**: 4320.
7. Lachowicz-Scroggins ME, Dunican EM, Charbit AR *et al*. Extracellular DNA, neutrophil extracellular traps, and inflammasome activation in severe asthma. *Am J Respir Crit Care Med* 2019; **199**: 1076–1085.
8. Wan H, Winton HL, Soeller C *et al*. Der p 1 facilitates transepithelial allergen delivery by disruption of tight junctions. *J Clin Invest* 1999; **104**: 123–133.
9. Takai T, Ikeda S. Barrier dysfunction caused by environmental proteases in the pathogenesis of allergic diseases. *Allergol Int* 2011; **60**: 25–35.
10. Georas SN, Rezaee F. Epithelial barrier function: at the front line of asthma immunology and allergic airway inflammation. *J Allergy Clin Immunol* 2014; **134**: 509–520.
11. de Boer WI, Sharma HS, Baelemans SM, Hoogsteden HC, Lambrecht BN, Braunstahl GJ. Altered expression of epithelial junctional proteins in atopic asthma: possible role in inflammation. *Can J Physiol Pharmacol* 2008; **86**: 105–112.
12. Tan H-T, Hagner S, Ruchti F *et al*. Tight junction, mucin, and inflammasome-related molecules are differentially expressed in eosinophilic, mixed, and neutrophilic experimental asthma in mice. *Allergy* 2019; **74**: 294–307.
13. Xiao C, Puddicombe SM, Field S *et al*. Defective epithelial barrier function in asthma. *J Allergy Clin Immunol* 2011; **128**: 549–556 e541–e512.
14. Persson C. Airways exudation of plasma macromolecules: innate defense, epithelial regeneration, and asthma. *J Allergy Clin Immunol* 2019; **143**: 1271–1286.
15. Carriere V, Roussel L, Ortega N *et al*. IL-33, the IL-1-like cytokine ligand for ST2 receptor, is a chromatin-associated nuclear factor *in vivo*. *Proc Natl Acad Sci USA* 2007; **104**: 282–287.
16. Schmitz J, Owyang A, Oldham E *et al*. IL-33, an interleukin-1-like cytokine that signals via the IL-1 receptor-related protein ST2 and induces T helper type 2-associated cytokines. *Immunity* 2005; **23**: 479–490.
17. Lefrancais E, Roga S, Gautier V *et al*. IL-33 is processed into mature bioactive forms by neutrophil elastase and cathepsin G. *Proc Natl Acad Sci USA* 2012; **109**: 1673–1678.
18. Lefrancais E, Duval A, Mirey E *et al*. Central domain of IL-33 is cleaved by mast cell proteases for potent activation of group-2 innate lymphoid cells. *Proc Natl Acad Sci USA* 2014; **111**: 15502–15507.
19. Watanabe M, Takizawa H, Tamura M *et al*. Soluble ST2 as a prognostic marker in community-acquired pneumonia. *J Infect* 2015; **70**: 474–482.
20. Xia J, Zhao J, Shang J *et al*. Increased IL-33 expression in chronic obstructive pulmonary disease. *Am J Physiol Lung Cell Mol Physiol* 2015; **308**: L619–L627.
21. Oshikawa K, Kuroiwa K, Tago K *et al*. Elevated soluble ST2 protein levels in sera of patients with asthma with an acute exacerbation. *Am J Respir Crit Care Med* 2001; **164**: 277–281.
22. Watanabe M, Nakamoto K, Inui T *et al*. Serum sST2 levels predict severe exacerbation of asthma. *Respir Res* 2018; **19**: 169.
23. Celedón JC, Milton DK, Ramsey CD *et al*. Exposure to dust mite allergen and endotoxin in early life and asthma and atopy in childhood. *J Allergy Clin Immunol* 2007; **120**: 144–149.
24. Michel O, Kips J, Duchateau J *et al*. Severity of asthma is related to endotoxin in house dust. *Am J Respir Crit Care Med* 1996; **154**: 1641–1646.
25. Daan de Boer J, Roelofs JJTH, de Vos AF *et al*. Lipopolysaccharide inhibits Th2 lung inflammation induced by house dust mite allergens in mice. *Am J Respir Cell Mol Biol* 2013; **48**: 382–389.

26. Krishnamoorthy N, Douda DN, Brüggemann TR *et al*. Neutrophil cytoplasts induce T_H17 differentiation and skew inflammation toward neutrophilia in severe asthma. *Sci Immunol* 2018; **3**: eaao4747.
27. Cummins PM. Occludin: one protein, many forms. *Mol Cell Biol* 2012; **32**: 242–250.
28. Frank JA. Claudins and alveolar epithelial barrier function in the lung. *Ann N Y Acad Sci* 2012; **1257**: 175–183.
29. Clark SR, Ma AC, Tavener SA *et al*. Platelet TLR4 activates neutrophil extracellular traps to ensnare bacteria in septic blood. *Nat Med* 2007; **13**: 463–469.
30. Jin R, Xu J, Gao Q *et al*. IL-33-induced neutrophil extracellular traps degrade fibronectin in a murine model of bronchopulmonary dysplasia. *Cell Death Discov* 2020; **6**: 33.
31. Neubert E, Senger-Sander SN, Manzke VS *et al*. Serum and serum albumin inhibit *in vitro* formation of neutrophil extracellular traps (NETs). *Front Immunol* 2019; **10**: 12.
32. Luzina IG, Pickering EM, Kopach P *et al*. Full-length IL-33 promotes inflammation but not Th2 response *in vivo* in an ST2-independent fashion. *J Immunol* 2012; **189**: 403–410.
33. Becker S, Quay J, Koren HS, Haskill JS. Constitutive and stimulated MCP-1, GRO alpha, beta, and gamma expression in human airway epithelium and bronchoalveolar macrophages. *Am J Physiol* 1994; **266**: L278–L286.
34. Li Y, Imaizumi T, Matsumiya T *et al*. Polyinosinic-polycytidylic acid induces CXCL1 expression in cultured hCMEC/D3 human cerebral microvascular endothelial cells. *Neuroimmunomodulation* 2020; **27**: 38–47.
35. Alves-Filho JC, Sônego F, Souto FO *et al*. Interleukin-33 attenuates sepsis by enhancing neutrophil influx to the site of infection. *Nat Med* 2010; **16**: 708–712.
36. Michaudel C, Mackowiak C, Maillet I *et al*. Ozone exposure induces respiratory barrier biphasic injury and inflammation controlled by IL-33. *J Allergy Clin Immunol* 2018; **142**: 942–958.
37. Fanny M, Nascimento M, Baron L *et al*. The IL-33 receptor ST2 regulates pulmonary inflammation and fibrosis to bleomycin. *Front Immunol* 2018; **9**: 1476.
38. Pham DL, Ban G-Y, Kim S-H *et al*. Neutrophil autophagy and extracellular DNA traps contribute to airway inflammation in severe asthma. *Clin Exp Allergy* 2017; **47**: 57–70.
39. Vermeer PD, Denker J, Estin M *et al*. MMP9 modulates tight junction integrity and cell viability in human airway epithelia. *Am J Physiol Lung Cell Mol Physiol* 2009; **296**: L751–L762.
40. Zhou Z, Yan F, Liu O. Interleukin (IL)-33: an orchestrator of immunity from host defence to tissue homeostasis. *Clin Transl Immunol* 2020; **9**: e1146.
41. Hong H, Liao S, Chen F, Yang Q, Wang DY. Role of IL-25, IL-33, and TSLP in triggering united airway diseases toward type 2 inflammation. *Allergy* 2020; **75**: 2794–2804.
42. Grünig G, Corry DB, Reibman J, Wills-Karp M. Interleukin 13 and the evolution of asthma therapy. *Am J Clin Exp Immunol* 2012; **1**: 20–27.
43. Patel DF, Peiró T, Bruno N *et al*. Neutrophils restrain allergic airway inflammation by limiting ILC2 function and monocyte-dendritic cell antigen presentation. *Sci Immunol* 2019; **4**: aax7006.
44. O'Byrne PM, Metev H, Puu M *et al*. Efficacy and safety of a CXCR2 antagonist, AZD5069, in patients with uncontrolled persistent asthma: a randomised, double-blind, placebo-controlled trial. *Lancet Respir Med* 2016; **4**: 797–806.
45. Brint EK, Xu D, Liu H *et al*. ST2 is an inhibitor of interleukin 1 receptor and Toll-like receptor 4 signaling and maintains endotoxin tolerance. *Nat Immunol* 2004; **5**: 373–379.
46. Sabroe I, Jones EC, Whyte MK, Dower SK. Regulation of human neutrophil chemokine receptor expression and function by activation of Toll-like receptors 2 and 4. *Immunology* 2005; **115**: 90–98.
47. Augustine J, Pavlou S, Ali I *et al*. IL-33 deficiency causes persistent inflammation and severe neurodegeneration in retinal detachment. *J Neuroinflammation* 2019; **16**: 251.
48. Swamydas M, Lionakis MS. Isolation, purification and labeling of mouse bone marrow neutrophils for functional studies and adoptive transfer experiments. *J Vis Exp* 2013; **77**: e50586.
49. Dobbs LG, Gonzalez R, Williams MC. An improved method for isolating type II cells in high yield and purity. *Am Rev Respir Dis* 1986; **134**: 141–145.

Supporting Information

Additional supporting information may be found online in the Supporting Information section at the end of the article.